Potential improvements of landslide prediction by hydro-meteorological thresholds: an investigation based on reanalysis soil moisture data and principal component analysis

Nunziarita Palazzolo[1], David J. Peres[2], Enrico Creaco[3], Antonino Cancelliere[2]

5 [1]Department of Civil Engineering and Architecture, University of Pavia, Italy, now at Department of Civil Engineering and Architecture, University of Catania, Catania, 95123, Italy.
[2] Department of Civil Engineering and Architecture, University of Catania, Catania, 95123, Italy.
[3] Department of Civil Engineering and Architecture, University of Pavia, Pavia, 27100, Italy.

10 *Correspondence to*: Nunziarita Palazzolo (nunziarita.palazzolo@unict.it)

Abstract. In recent times, several efforts have been addressed to understand the extent to which soil moisture estimations may improve the performance of landslide early warning systems (LEWSs). These systems have been traditionally based on rainfall intensity-duration thresholds. Still a limited number of studies explore the possible enhancement of the performance of LEWSs through the identification of hydro-meteorological thresholds. In this study, we propose a

15 methodology for developing regional hydro-meteorological landslide triggering thresholds coupling mean rainfall intensity and soil moisture information. To test the potential improvements in prediction we use ERA5-Land reanalysis soil moisture data, available at four depth levels and hourly resolution. Two different instances are investigated, namely the identification of triggering thresholds using rainfall intensity and the soil moisture at each of four depth levels, and the identification of triggering thresholds using rainfall intensity and a combination of soil moisture at the four depths as

20 obtained by principal component analysis (PCA). We propose thresholds in the form of a piece-wise linear equation. The equation's parameters are optimized in order to maximize the ROC True Skill Statistic (TSS) prediction performance metric. The proposed hydro-meteorological thresholds are tested on the case of Sicily Island (south Italy) and the performance is compared with those obtained through the traditional rainfall intensity-duration (ID) power-law thresholds. Overall, the results show that the soil moisture information adds a considerable value to the improved thresholds'

25 performance since the ROC True Skill Statistic increases from 0.50 to 0.71. A similar performance is obtained when the first principal component derived from the PCA is used, proving PCA to be a valuable support tool for the identification of the proposed hydro-meteorological thresholds, as it allows to take into account the multi-layer information while keeping the thresholds two-dimensional.

30

1 Introduction

The impact of landslides triggered by rainfall, is constantly increasing due to landscape modifications, i.e. urbanization,
35 deforestation, land-changes and the abandonment of rural areas (Roccati et al., 2019). They can cause serious damage to
man-made structures and land, as well as loss of natural resources and lives (Froude and Petley, 2018). Furthermore, in the
last decades, an increasing number of studies focused on the potential effects of climate change on landslide phenomena
(McInnes et al. 2007; Dijkstra and Dixon 2010; Crozier 2010), pointing out that there are some unresolved issues, such as
the abundance, activity, frequency and return period of landslides in response to the projected climate change (Gariano and
40 Guzzetti, 2016; Peres and Cancelliere, 2018). In light of these considerations and, after recent catastrophic landslides
worldwide, there is a high interest of scholars and civil protection agencies in the development of landslide early warning
systems (LEWS), which can serve as an aid in predicting possible slope movements, and thus as risk mitigation tool (Roccati
et al., 2020; Highland and Bobrowsky, 2008; Chae et al., 2017).

Landslide triggering thresholds are a key component of LEWS. In general, even if LEWS vary widely in approaches and
45 scale, empirical rainfall thresholds in combination with rainfall measurements and forecasts remain the most frequently
applied approaches for the majority of regional LEWSs. In the literature, several methods have been proposed for the
identification of rainfall thresholds to landslides initiation (Guzzetti et al., 2007a, 2008; Segoni et al., 2018a; Aleotti, 2004).
Empirical rainfall thresholds are usually obtained by drawing lower-bound lines to the rainfall conditions inducing
landslides, plotted in Cartesian, semi-logarithmic, or logarithmic coordinates (e.g., rainfall duration on the abscissa axis and
50 rainfall intensity on the vertical axis). When information on non-triggering rainfall is also available, thresholds can be
determined as the best classifiers based on the confusion matrix (Berti et al., 2012; Staley et al., 2013; Peres and Cancelliere,
2014; Postance et al., 2018; Marino et al., 2020; Peres and Cancelliere, 2021).

Commonly, these rainfall exceedance thresholds empirically relate the occurrence of landslides to rainfall event
characteristics such as intensity, duration, total amounts, or a combination thereof (Wicki et al., 2020a). However, in many
55 settings the antecedent soil wetness conditions influence the variability in rainfall triggering amounts, becoming a
predisposing factor that plays a major role in landslide initiation (Palau et al., 2021; Conrad et al., 2021). This led to a more
recent approach that relies not only on rainfall but, also, on subsurface hydrological measurements (e.g. soil moisture
content), thus introducing hydro-meteorological thresholds (Mirus et al., 2018b, a; Thomas et al., 2018; Segoni et al., 2018c;
Wicki et al., 2020a; Bogaard and Greco, 2018, 2016) for a better representation of landslide triggering. The term "hydro-
60 meteorological" is because these threshold combine a meteorological variable (rainfall depth) with a hydrological one,
reflecting the water storage at the catchment or local scale (Gain et al., 2021).

 In this regard, several attempts aimed at introducing, directly or with models, the effects of soil moisture information in the
empirical thresholds for improving landslide prediction have been made (Crozier, 1999; Zhao et al., 2019; Brocca et al.,
2016; Segoni et al., 2018c; Ponziani et al., 2012). For instance, Marino et al. (2020) performed an explorative numerical
65 investigation to understand whether soil moisture information can improve shallow landslide forecasting using the hydro-

meteorological threshold approach. In their work, they used synthetic rainfall and landslide data obtained through Monte Carlo simulation. Their results showed that soil moisture information introduced within hydro-meteorological thresholds can significantly reduce the false alarm ratio of LEWS, while keeping at least unvaried the number of missed alarms. Along this path, Reder and Rianna (2021) addressed the extent to which soil moisture estimations can be useful to define a proxy for

70   antecedent slope wetness conditions. In particular, they used the soil moisture data derived from the ERA5-Land reanalysis (Hersbach et al., 2020) as a support for LEWS, and more specifically as an initial filter for a pre-screening of the effective saturation degree. They showed that the filter yielded by the ERA5 soil model is able to strengthen the regional warning system and that the ERA5 reanalysis provides estimations consistent with those retrieved by using more complex and detailed physically based models.

75   Lastly, Wicki et al. (2021) compared the reliability of landslides forecast models based on simulated soil moisture with respect to models based on soil moisture measurements. Specifically, they assessed the potential and limitations of adopting 1D soil water transfer model for regional LEWS and disclosed the pros and cons compared of using soil moisture measurements. To this aim, they used plot-scale soil hydrological simulations to be able to directly compare the results to a landslide forecast model based on in situ soil moisture measurements and demonstrated a high information content of

80   simulated soil moisture for regional landslide activity, which was even higher than when in situ soil moisture measurements were used (Wicki et al., 2021). In this regard, Wicki et al. (2020b), demonstrated that the performance is strongly dependent on the distance between the soil moisture network location and landslide activity area and that the goodness increases with decreasing distances between measurement sites and landslides. Therefore, the density of the soil moisture measurement networks impacts the performance of a LEWS and these measurement networks should consider the spatial variability of

85   meteorological events and soil properties (Wicki et al., 2020b).

In light of these advances, in the present work we attempt to give a further contribution by investigating the possible improvements of landslide prediction through hydro-meteorological thresholds coupling observed rainfall intensity and soil moisture information. In particular, we carry out our investigation considering the ERA5-Land reanalysis data set. In fact, recent studies proved that the main climate variables (i.e., soil moisture, temperature, precipitation) obtained from third-

90   generation atmospheric and reanalysis datasets, (i.e., ERA5 project) have a reasonable accuracy in reproducing in situ-measurements of the reference local weather stations from the International Soil Moisture Network (Dorigo et al., 2011; Li et al., 2020; Beck et al., 2021).

A real case study is used to test the methodology, obtained by joining, over the period 2010-2018, the dataset of observed landslide and rainfall events with the dataset of soil moisture values reconstructed by the ERA5-Land reanalysis at the

95   beginning of rainfall events. The proposed methodology involves the identification of the equation describing the threshold through a heuristic approach and an optimization procedure aimed at finding the optimal values of its parameters, in order to maximize the ROC True Skill Statistic (TSS). In order to combine the information of multiple layers of soil moisture data availability, ~~the~~ Principal Component Analysis (PCA) (Jolliffe, 2002) is used, a multivariate statistical tool which capitalizes on the presence of correlation between the soil moisture at different depths. Thus, two different instances are investigated,

100   namely the identification of four triggering thresholds using the rainfall intensity and the soil moisture at each of four depth
         levels, and the identification of the triggering threshold using the rainfall intensity and first principal component of soil
         moisture at all four depths.

         The paper is organized as ~~follow~~. First the procedure for the dataset creation and the methodology leading to the hydro-
         meteorological thresholds identification are presented in the "Material and Methods" section. Then, the "Study Area" section
105   describes the relevant features of the study area, namely the Sicily Island (Southern Italy). Next, the results and discussion
         concerning the comparison between the performance obtained through the traditional ID thresholds and the proposed hydro-
         meteorological thresholds, are presented in the "Results and Discussion" section. Finally, conclusions are drawn in the last
         section.

2 Materials and method

110   ### 2.1 Dataset construction

         The construction of a rainfall and landslide events dataset is a key step, which involves different types of data (i.e., observed
         landslides, rainfall events and, reanalysis data of soil moisture). As schematically illustrated in Fig. 1, in the first step,
         information is collected regarding the observed landslides from the FraneItalia project (Calvello and Pecoraro, 2018), a
         thorough spatio-temporal inventory of historical landslides that have impacted the Italian territory since 2010, including both
115   occurrences that resulted in fatalities and occurrences that did not.
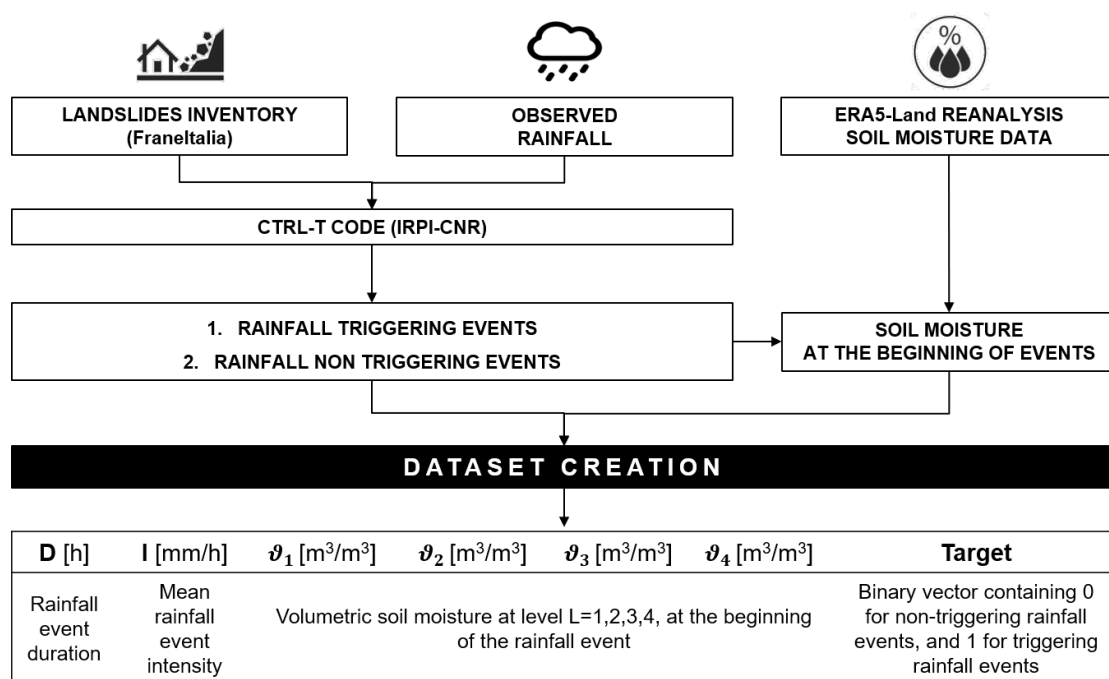
Figure 1: Schematization of the procedure followed for dataset construction.

The first classification criterion by the FraneItalia catalogue is based on the number of landslides triggered by the same rainfall event in a given geographic area. Specifically, single landslide events (SLE) and areal landslide events (ALE) are

120   distinguished for records referring to single or multiple landslides, respectively. Both SLEs and ALEs are then categorized into one of three classes in relation to their impacts, in order to track whether a landslide occurrence resulted in casualties or missing people (C1, very severe), injured people and evacuations (C2, severe), or no one was physically harmed (C3, minor). The data on occurrence location, the date the landslide occurred, the source of information, and the number of landslides for ALEs are further details that have been also included in the catalogue, together with the onset and duration of the landslide

125   occurrence and its consequences.

Thanks to this accurate level of detail, it is possible to filter only the landslide events triggered by rainfall, which are precisely those to take into consideration in our study.

The CTRL-T (Calculation of Thresholds for Rainfall-induced Landslides-Tool) code (Melillo et al., 2018) is subsequently used for the identification of the rainfall events that were more likely to be responsible for the observed slope failures.

130   Specifically, CTRL-T automatically and objectively reconstructs rainfall events and the triggering conditions responsible for the failure using a set of adjustable parameters to account for different morphological and climatic settings. Briefly, the tool consists of distinct modules with specific purposes. Among these, one module operates the reconstruction of rainfall events in term of duration (D, in hours) and, cumulated event rainfall (E, in mm) using continuous hourly rainfall time series and setting several climate and spatial parameters such as, the warm period in a year (C_W); the cold period in a year (C_C); the

135   resolution of the rain gauge (G_S); time periods used to remove irrelevant amount of rain and to reconstruct rainfall events (P_1, P_2, P_4); irrelevant rainfall sub-events that had to be excluded in the calculation of the final events (P_3); radius of the buffer to assign each landslide to the closest rain gauge (R_B). Rainfall event parameters were calibrated adopting the monthly soil water balance model and evapotranspiration analysis. A further module, instead, performs selection of the rain gauge representative for the landslide. The maximum allowed distance between a landslide and a rain gauge is limited by the

140   circumferential area with radius equal to R_B. Single or multiple rainfall conditions (MRC) that are most likely responsible for the slope failures are, then, identified. MRC can be a (D_L, E_L) pair of rainfall event duration (D_L) and cumulated event rainfall (E_L), or a set of two or more pairs. Each MRC is assigned a weight to select the representative rain gauge and the rainfall conditions associated with the landslide. The weight is proportional to the inverse square distance between the rain gauge and the landslide (d^{-2}), the cumulated rainfall (E_L), and the rainfall mean intensity ($E_L D_L^{-1}$):

145    $$w = f(d, E_L, D_L) = d^{-2} E_L^2 D_L^{-1} \qquad (1)$$

Thus, among all the identified MRCs, those with the highest weights w are defined as the maximum probability rainfall conditions (MPRCs) and, ~~precisely~~ these reconstructed rainfall conditions were assumed as the rainfall triggering events. The landslides for which the rainfall conditions were not identified or with relevant uncertainties~~,~~ were discarded.

As shown in Fig. 1, the last step for the dataset set up consists of the association of soil moisture data to the beginning of

150   each rainfall event, both triggering and non-triggering ones. In this regard, the ERA5-Land reanalysis dataset is used. ~~Indeed,~~

it provides the volume of water ϑ [m³/m³] at four distinct soil depths levels (i.e., 0-7 cm; 7-28 cm; 28-100 cm, and 100-289 cm). The ERA5-Land soil moisture data are provided as grid data with a horizontal resolution of 0.1° x 0.1°. Thus, the soil moisture values representative of the closest cell to the rain gauge that recorded the rainfall event are associated to the considered event. Thereby, the dataset in the form shown in Fig. 1, was created.

2.2 Principal component analysis

Principal Components Analysis (PCA) (Jolliffe, 2002) is a multivariate technique that analyzes a data table in which observations are described by several inter-correlated quantitative dependent variables in order to extract the important information from the table and, to represent it as a set of new orthogonal variables called principal components (Abdi and Williams, 2010).

Precisely, the data are transformed according to a new coordinate system having the x-axis, known as the first principal axis, characterized by the highest data variation. Along the successive ~~after~~ axes (e.g., the second principal axis, the third principal axis, and so on) the data are characterized by increasingly lower variation. ~~Indeed, up until the entire data table is reduced,~~ each succeeding principal component explains the maximum amount of variance feasible with the requirement that it is orthogonal to the previous principal components. In practice, identifying the eigenvalues and eigenvectors of the covariance matrix is the formal mathematical equivalent of solving the PCA problem. ~~Indeed,~~ the direction along which the data have the highest variance is the eigenvector, while, the related eigenvalue is a quantification of the variance in the data along the corresponding eigenvector. Accordingly, the first principal component is the eigenvector with the greatest eigenvalue, followed by the eigenvector with the second-highest eigenvalue, and so on. Thus, the so computed principal components are employed for the projection of the data into the new coordinate space (Kherif and Latypova, 2019).

Practically, in our study, $\boldsymbol{\theta}$ (Eq. 2) represents the soil moisture data table for which to compute the principal components, specified as an n-by-p matrix. Rows correspond the total amount n of the considered rainfall events (i.e., observations), and the number of columns to the four depths levels at which the initial soil moisture data are provided (i.e., variables).

$$\boldsymbol{\theta} = \begin{bmatrix} \vartheta_{11} & \vartheta_{12} & \vartheta_{13} & \vartheta_{14} \\ \vartheta_{21} & \vartheta_{22} & \vartheta_{23} & \vartheta_{24} \\ \vdots & \vdots & \vdots & \vdots \\ \vartheta_{n1} & \vartheta_{n2} & \vartheta_{n3} & \vartheta_{n4} \end{bmatrix} \tag{2}$$

$\boldsymbol{A}$ represents, instead, the principal components' loadings (i.e., coefficients) table, specified as an p-by-p matrix. The rows of matrix A are called the eigenvectors, and these specify the orientation of the principal components relative to the original variables.

$$\boldsymbol{A} = \begin{bmatrix} a_{11} & a_{12} & a_{13} & a_{14} \\ a_{21} & a_{22} & a_{23} & a_{24} \\ a_{31} & a_{32} & a_{33} & a_{34} \\ a_{41} & a_{42} & a_{43} & a_{44} \end{bmatrix} \tag{3}$$

Thus, the principal components (S_i) for the generic i_{th} row, are given by a linear combination of the variables $\boldsymbol{\theta}$ and $\boldsymbol{A}$, namely:

$$S_{i1} = a_{11}\vartheta_{i1} + a_{12}\vartheta_{i2} + a_{13}\vartheta_{i3} + a_{14}\vartheta_{i4} \tag{4}$$

$$S_{i2} = a_{21}\vartheta_{i1} + a_{22}\vartheta_{i2} + a_{23}\vartheta_{i3} + a_{24}\vartheta_{i4} \tag{5}$$

$$S_{i3} = a_{31}\vartheta_{i1} + a_{32}\vartheta_{i2} + a_{33}\vartheta_{i3} + a_{34}\vartheta_{i4} \tag{6}$$

$$S_{i4} = a_{41}\vartheta_{i1} + a_{42}\vartheta_{i2} + a_{43}\vartheta_{i3} + a_{44}\vartheta_{i4} \tag{7}$$

with $i = 1, ..., n$.

In matrix notation, the transformation of the original variables to the principal components is written as,

$$\boldsymbol{S} = \boldsymbol{\theta A} \tag{8}$$

2.3 Threshold identification

The methodology adopted in this work aims to improve the identification of regional landslides triggering thresholds by means of reanalysis soil moisture information and, to compare the obtained performance with those obtained through the traditional rainfall intensity-duration power-law thresholds (*ID*). Therefore, the rainfall intensity-duration threshold, the most common type of threshold proposed and adopted in the literature (Segoni et al., 2018b; Guzzetti et al., 2007b; Brunetti et al., 2010), is used as benchmark. The *ID* threshold assumes the form $I = \alpha D^{-\beta}$, where I [mm/h] represents the rainfall intensity, i.e., the average precipitation rate over the considered period; D [h] represents the duration of the rainfall event; α is the intercept parameter, and β is the slope parameter. After reconstructing the rainfall events with the methodology explained for the dataset creation and, after calculating the main variables (i.e., mean rainfall intensity and duration), an optimization tool (i.e., the MATLAB® Particle Swarm optimization toolbox) is used with the aim to search for the best possible α and β curve parameters able to maximize the True Skill Statistic index (TSS) objective function (Eq. 11), which is based on the confusion matrix or the Receiver-Operating Characteristics (ROCs). The confusion matrix is expressed in terms of the count of true positives (TP), true negatives (TN), false positives (FP) and false negatives (FN) (Peirce, 1884) (Table 1).

Table 1: Confusion matrix for ROC analysis.

		Observed landslide	
		Landslide (P)	No landslide (N)
Predicted Landslide	Landslide	TP	FP
	No landslide	FN	TN

As a function of the variables reported in Table 1, the three reference standard ROC indices – namely, True Positive Rate, False Positive Rate and True Skill Statistic – are listed below (Eqs. 9, 10, 11):

$$TPR = \frac{TP}{(TP + FN)} \tag{9}$$

$$FPR = \frac{FP}{(TN + FP)} \tag{10}$$

$$TSS = TPR - FPR \tag{11}$$

The highest performances correspond to TSS = 1, when, relatively to a given rainfall event, the model produces no false or missing predictions.

Afterward, the analysis is focused on the identification of the parametric equation that represents the lower boundary
210 between triggering and no-triggering rainfall events on the basis of the mean rainfall intensity and the reanalysis of soil moisture values at each depth level. In this context, we propose the following parametric threshold as a reliable relationship to classify the events on the semi-log plane:

$$I = \begin{cases} y_0, & \vartheta < x_0 \\ \dfrac{y_1 - y_0}{x_1 - x_0}(\vartheta - x_0) + y_0, & x_0 \leq \vartheta \leq x_1 \\ y_1, & \vartheta > x_1 \end{cases} \tag{12}$$

where I and ϑ correspond to rainfall intensity and to soil moisture values, respectively. This parametric form of the threshold
215 has been devised based on the visual inspection of the scatter plot of triggering and non-triggering events (i.e., heuristically), and corroborated by comparison with other relationships proposed in the literature – specifically, the power-law and the simple bilinear (as opposed to a linear or more complex power or high-degree polynomial) (Thomas et al., 2019; Mirus et al., 2018a). Furthermore, x_0, x_1, y_0, and y_1 are the threshold's parameters that must be estimated. In this regard, these parameters are computed by adopting the same objective function and optimization procedure as those used for the
220 identification of the parameters of the power-law ID threshold, i.e., the True Skill Statistic index (TSS) objective function (Eq. 11) and the MATLAB® Particle Swarm global optimization toolbox. At this stage, the threshold identification methodology described so far is applied with the aim to identify triggering thresholds between the mean rainfall intensity (I) and the soil moisture expressed in two variants: *i*) soil moisture at each of the four depth levels ($\vartheta_1, \vartheta_2, \vartheta_3, \vartheta_4$) available from the ERA 5 - reanalysis; *ii*) the first principal component of soil moisture, i.e. the linear combination of soil moisture at the
225 four depths corresponding to the minimum information loss (highest explained variance). The TSS values obtained in the applications considering soil moisture (hereinafter indicated as TSS_{par}) were compared with the TSS values obtained for the reference scenario of the power-law ID threshold (hereinafter TSS_{pl}).

3 Study area

The study area selected for our study is the island of Sicily (southern Italy, 37.75N-14.25 E) which, with an area of
230 ~25,700 km², is the largest island of the Mediterranean Sea. A hilly morphology (62%) dominates the landscape in the island, while the rest is characterized by a mountainous and flat morphology, especially in the eastern part of the island around Catania. The terrain average elevation is about 400 meters above sea level, ranging from 0 to 3320 meters on the peak of the Etna volcano. Geologically, the Sicily Island arose during the Neogene, when the European and African plates converged. Thus, Sicily stands out for its complex geological and lithological features which, cooperatively with anthropic
235 activities (e.g., changes in land use, management of forest, etc.), have generated a wide range of different types of soil (Venturella, 2004).

The climate is warm-temperate, with hot and dry summers, especially on the southern coasts, and higher and more frequent precipitation during the colder winter months, in the mountainous internal areas (Pumo et al., 2019). Mean annual precipitation ranges between 700 and 800 mm and, autumn and winter are the rainiest seasons. The most severe rainfall

240   events frequently hit the eastern side of the island and specifically, the eastern side of the Etna volcano and the flanks of the Peloritani Mountains, with the greatest precipitation peaks on the Ionian side (Gariano et al., 2015). On the other hand, south Sicily is distinguished by lower precipitation than the mean values recorded in the rest of the region, since it is located at a lower height and is exposed to the hot and dry African winds (Alecci and Rossi, 2007).

Fig. 2 shows the geographical context of Sicily, the rain gauge locations for the period 2009-2018 (Distefano et al., 2021)

245   and the observed landslide locations. In more detail, 207 landslide events were retrieved by the FraneItalia database from 2010 to 2018 and, for each of them, longitude-latitude coordinates (WGS84 datum), together with the initiation time, are retrieved.
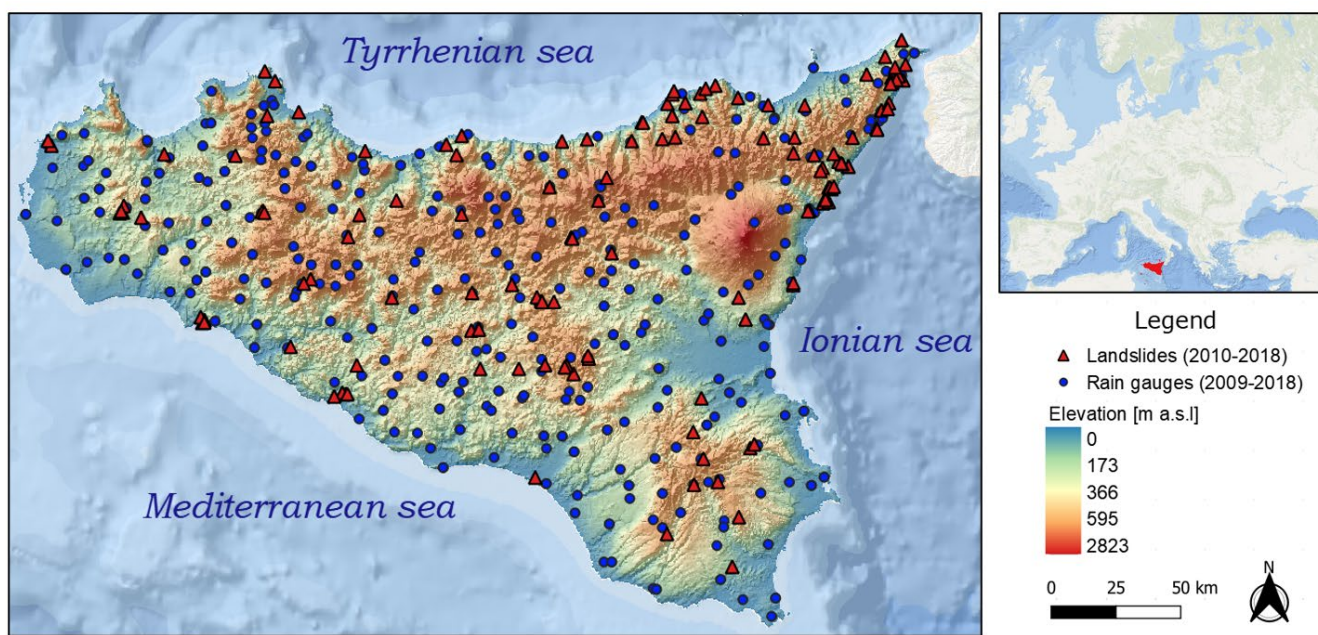
Figure 2: Elevation map of the study area (Sicily region), showing the location of the rain gauges and landslide occurrences.
250   **(Credit to: http://www.sinanet.isprambiente.it/it/sia-ispra/download-mais and ESRI 2020).**

Concerning the observed rainfall measurements, we consulted the data provided by the regional water observatory (Osservatorio delle Acque, OdA), the SIAS (Sicilian Agro-meteorological Information Service), and the Regional Civil Protection Department (DRPC), namely the three main gauging networks installed in Sicily.

This enabled an hourly time series to be reconstructed for the precipitation over the period 2009-2018. As previously

255   explained in Section 2.1, using these continuous rainfall time series, the rainfall events were identified using the CTRL-T research code. Specifically, the minimum dry period separating two rainfall events was set equal to 48 hours in the warm period C_W (April-October) and, equal to 96 hours in the cold period C_C (November- March).

4 Results and discussion

4.1 Principal Component Analysis

260 An explorative analysis was, initially, carried out, in order to investigate the correlation between the four soil moisture depths ($\vartheta_1, \vartheta_2, \vartheta_3, \vartheta_4$). The plot shown in Fig. 3 represents the correlation matrix between all pairs of variables, together with the Pearson's correlation coefficients.

Overall, all the four soil moisture depths are related to each other. Specifically, the diagonal subplot between the upper two depths levels ϑ_1 and ϑ_2 has the highest correlation with a correlation coefficient R equal to 0.85. This suggest that the

265 Principal Component Analysis can be adopted in order to find out the linear combination expressing the correlation between the involved soil moisture variables.
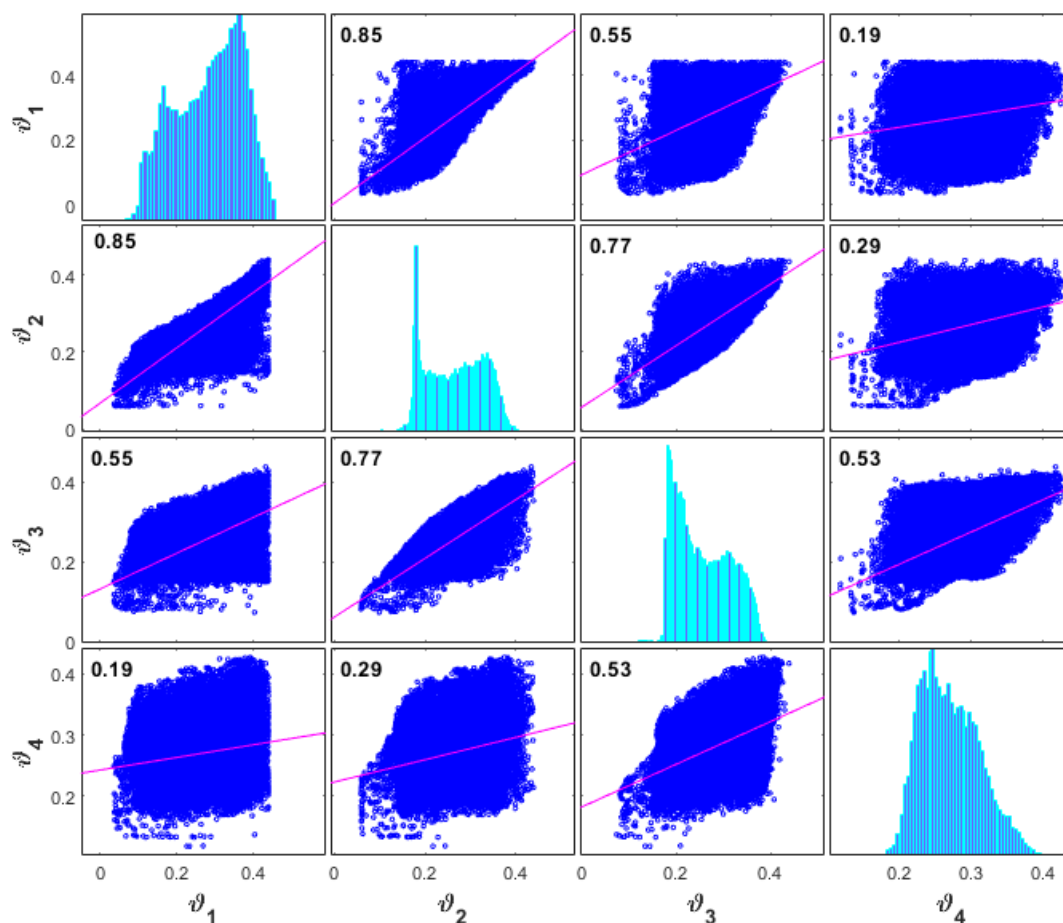
Figure 3: Correlation matrix between the four soil moisture level depths ($\vartheta_1, \vartheta_2, \vartheta_3, \vartheta_4$). Each off-diagonal subplot contains a scatterplot of a pair of variables with a least-squares reference line, the slope of which is equal to the displayed correlation
270 **coefficient. Each diagonal subplot contains the distribution of a variable as a histogram.**

The preliminary step, required when the principal component analysis is performed, is to center the data on the mean values of each variable, namely by subtracting the mean of a variable from all values of that variable. This step allows the cloud of data to be centered on the origin of the principal components, but it affects neither the spatial relationships of the data, nor the explained variance along the variables. At this stage, it was possible to proceed with the Principal Component Analysis and, according to Eqs. 4, 5, 6, and 7, the four principal components of soil moisture were defined as follow:

$$S_{i1} = 0.65\vartheta_{i1} + 0.58\vartheta_{i2} + 0.47\vartheta_{i3} + 0.15\vartheta_{i4} \tag{13}$$

$$S_{i2} = -0.54\vartheta_{i1} - 0.04\vartheta_{i2} + 0.63\vartheta_{i3} + 0.55\vartheta_{i4} \tag{14}$$

$$S_{i3} = 0.37\vartheta_{i1} - 0.29\vartheta_{i2} - 0.39\vartheta_{i3} + 0.79\vartheta_{i4} \tag{15}$$

$$S_{i4} = -0.38\vartheta_{i1} + 0.76\vartheta_{i2} - 0.48\vartheta_{i3} + 0.23\vartheta_{i4} \tag{16}$$

The loadings values of each principal component are intended as the weights a_{ij} (Eq. 3): therefore, the higher the value of the weight, the larger the contribution of a variable to the component associated with the weight. The sign of a loading indicates whether a variable and a principal component are positively or negatively correlated. Here, although overall slightly large loadings correspond to the first principal component, none of the four variables has a strong relationship with a particular principal component.

Fig. 4 shows, instead, the scree plot representing the total percentage of variance explained by each of the four principal components. The chart reveals the decreasing rate at which variance is explained by additional principal components.
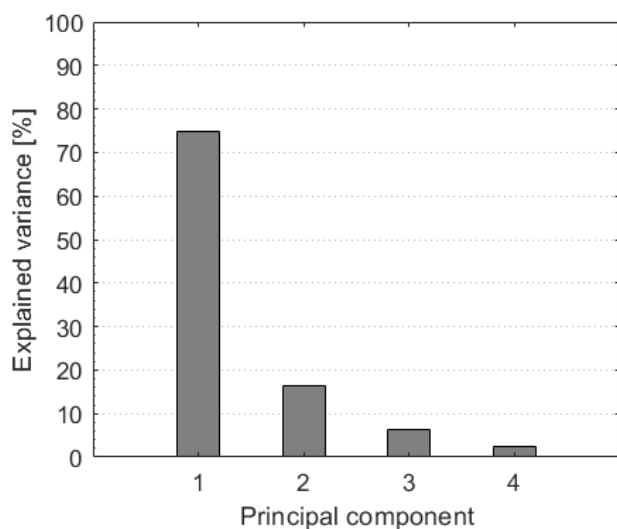
Figure 4: Total variance explained by each principal component.

Because dimensionality reduction is a goal of PCA, several criteria can be considered for determining how many principal components should be examined and how many should be ignored (Rencher, 1998). Just to list a few: *i*) ignore principal components at the point at which the next principal component offers little increase in the total explained variation; *ii*) ignore the last principal component whose explained variation are all roughly equal; *iii*) include all principal components up to a

predetermined total explained variation. In our study, the third criterion was applied considering a threshold value of 75%. Therefore, only the first principal component was considered as it guaranteed ~~by itself~~ the desired explained variation of

295   about 75 %.

4.2 Thresholds identification

CTRL-T tool reconstructed 144 landslide events out of the 207 landslides retrieved by the FraneItalia database. Four different triggering rainfall events, representing a range of triggering conditions, were selected within the database, and the precipitation time series together with the soil moisture time series are plotted in Fig. 5.
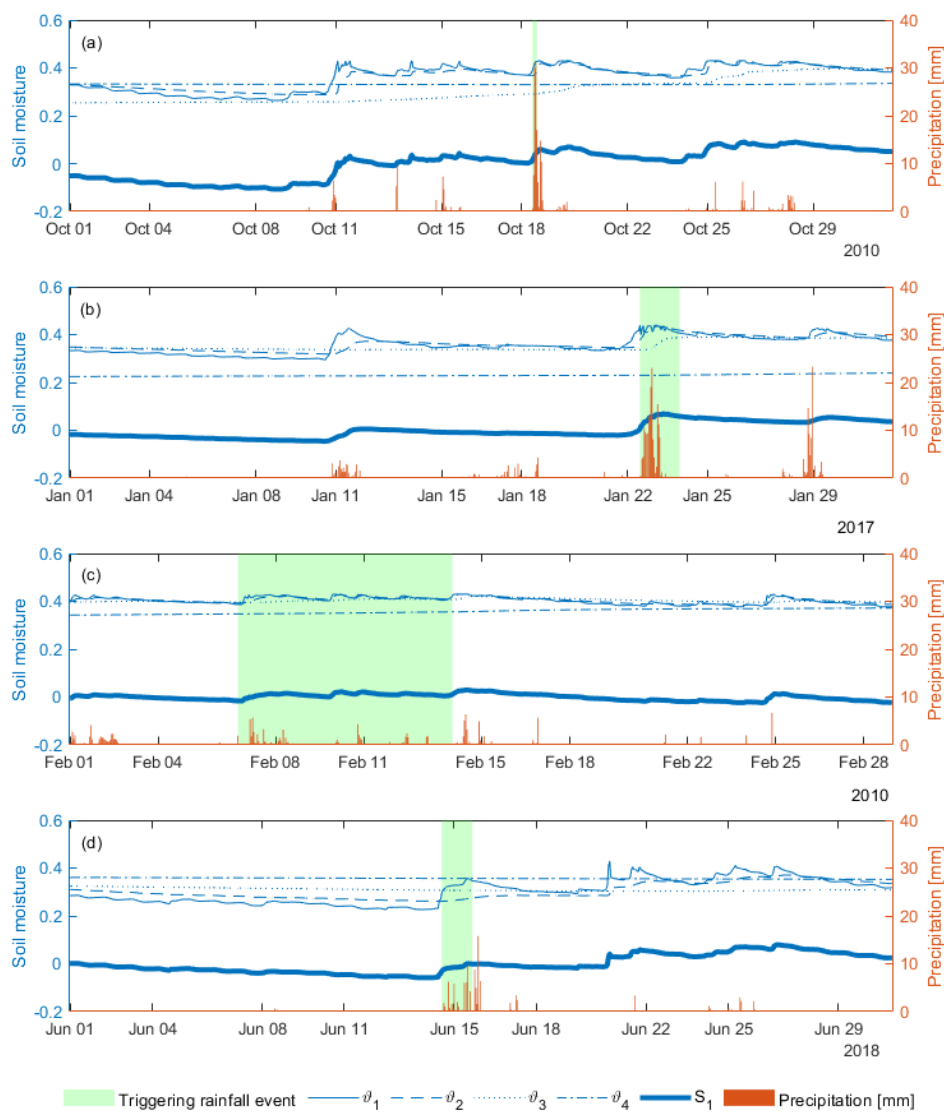
300   Figure 5: Panel showing four different triggering rainfall events. For each of them the precipitation time series together with the soil moisture time series (ϑ_1, ϑ_2, ϑ_3, ϑ_4) are reported, as well as the first principal component of soil moisture S_1.

The light green window, within each graph, represents the triggering rainfall event in relation to the wider window of the corresponding entire month. As expected, especially the upper two soil moisture layers reflect the precipitation trends, as
305 well as the first principal component of soil moisture S_1, computed using Eq. 13. Overall, a greater variability in soil moisture values can be observed in correspondence to ϑ_1 and ϑ_2, which assume maximum values about equal to 0.4 in correspondence of all the analyzed triggering rainfall events. Furthermore, Fig.5 shows as in correspondence of longer rainfall duration, lower precipitation values have triggered landslides (Fig.5 (c)) and vice-versa (Fig.5 (a)).

First, the power-law *ID* threshold maximizing TSS was identified (Fig. 6).
310
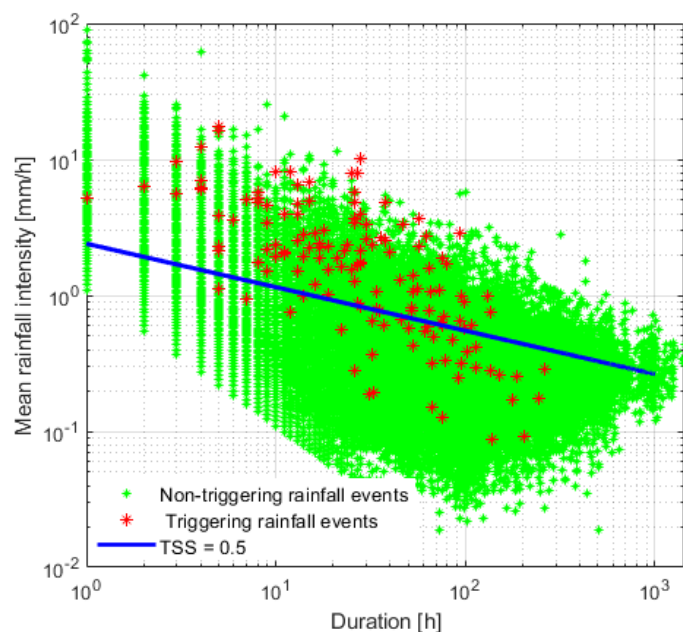
Figure 6: Traditional power-law threshold on the log-log plane between observed mean rainfall intensity (I) and duration (D).

For this threshold a $TSS_{pl} = 0.50$ is obtained, and this value was taken as benchmark for comparison with the hydro-meteorological thresholds constructed considering the two variants of hydro-meteorological thresholds described in
315 subsection 2.3. Fig. 7 shows the obtained thresholds when the mean rainfall intensity and the soil moisture at each of the four depth levels are considered. As can be seen, especially in correspondence to the upper two depths (i.e., 0-7 cm, 7-28 cm), the triggering rainfall events are located, for the most, on the right-upper side of the graph, suggesting that the equation proposed for the identification of the thresholds (Eq. 12) fits this trend well. All ~~the~~ four identified thresholds have better performance than *ID* threshold. Specifically, higher TSS values were obtained for the first two depths, with a TSS_{par} equal to 0.71 while
320 slightly lower values of TSS_{par} (0.61 and 0.54), are obtained with the third and fourth soil moisture level, respectively.
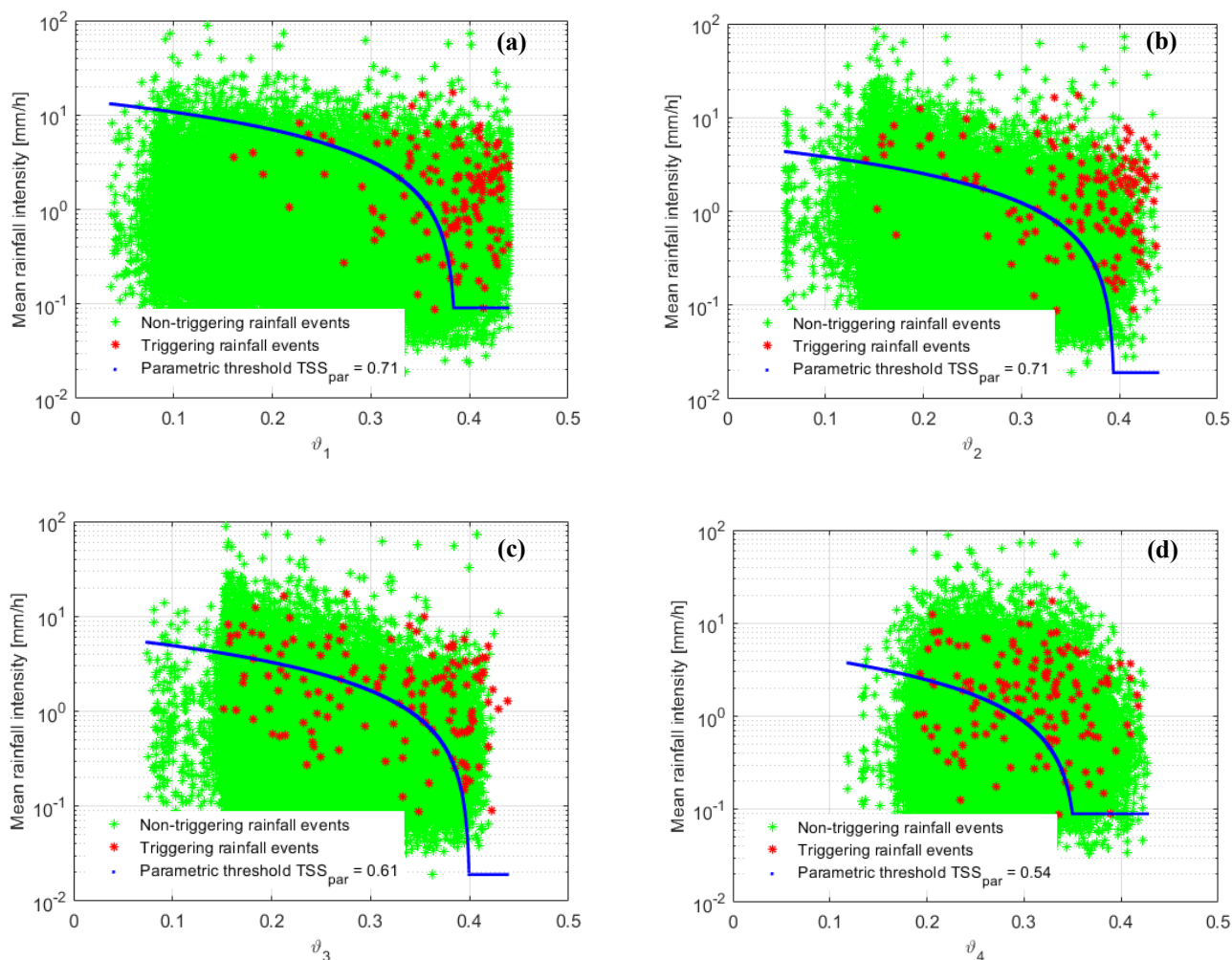
Figure 7: Parametric thresholds on the semi-log plane between mean rainfall intensity and soil moisture at the four distinct depths: (a) ϑ_1 0-7 cm; (b) ϑ_2 7-28 cm; (c) ϑ_3 28-100 cm; (d) ϑ_4 100-289 cm.

As ~~mentioned before,~~ the second analysis concerns the identification of the optimal parametric thresholds when the mean rainfall intensity and first principal component of soil moisture are considered (Fig. 8). In this variant, a $TSS_{par} = 0.71$ was

325 obtained once again, reaching an equal performance to the best case of the first variant and, thus, improved results in comparison with the *ID* approach.
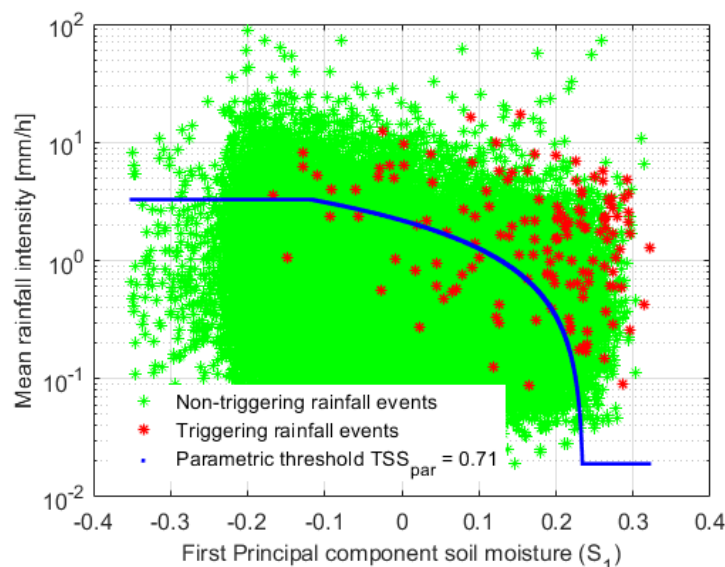
Figure 8: Parametric threshold on the semi-log plane between observed mean rainfall intensity (I) and first principal component of soil moisture (S_1).

330 Table 2 summarizes the *TSS* values in correspondence of the analyzed thresholds, together with the values of parameters (Eq. 12) estimated for the parametric thresholds.

Table 2: TSS values in correspondence to each analyzed scenario, and parameters (x_0, y_0, x_1, y_1) estimated for the parametric thresholds.

Threshold	TPR_{par}	FPR_{par}	TSS_{par}	x_0	y_0	x_1	y_1
$I\vartheta_1$	0.84	0.14	0.71	-0.33	27.23	0.38	0.09
$I\vartheta_2$	0.84	0.14	0.71	0.05	5.73	0.39	0.02
$I\vartheta_3$	0.73	0.12	0.61	-0.03	6.98	0.40	0.02
$I\vartheta_4$	0.79	0.25	0.54	-0.08	6.82	0.35	0.09
IS_1	0.85	0.14	0.71	-0.12	3.28	0.23	0.02

335 Overall, the proposed hydro-meteorological thresholds proved able to better predict the landslide occurrences, if compared with the performance of the traditional *ID* approach.

Indeed, the hydro-meteorological parametric threshold resulted in TSS_{par} values up to 0.71, confirming that considering soil moisture information in landslide triggering thresholds can significantly improve their predictive performance. As expected, the higher TSS values have been obtained in correspondence of the upper layers (ϑ_1, ϑ_2) for which there is the highest

340 correlation (Fig. 3).

Moreover, the study revealed that the inclusion of PCA allows obtaining a more generalized approach, which keeps unaltered the prediction performance while not requiring any prior identification of the most influential soil layer.

The parametric form proposed in this work in equation (12) was also compared with other more canonical expressions. Taking as reference variables the observed mean rainfall intensity (I) and first principal component of soil moisture (S_1), it

345 proved superior to the power-law threshold within the log-log plane and to the bi-linear threshold within the semi-log plane, which scored lower values of *TSS*, equal to 0.51 and 0.66, respectively. This highlights the importance of defining thresholds using an adequate parametric equation, as this choice can jeopardize the exploitation of soil moisture information for improving their prediction performance.

5 Conclusions

350 In this study, the potential improvements of regional landslide prediction by the use of soil moisture information and multi-variate statistical analysis (Principal component analysis) were explored, with reference to the case study of Sicily, Italy. For the investigation, we have used ERA5-Land reanalysis soil moisture information. The hydro-meteorological thresholds, combining precipitation and soil moisture information, proved better at classifying triggering and non-triggering rainfall events when compared to the traditional ID power-law thresholds. Specifically, a valuable improvement was found when the

355 upper layers of soil moisture are used for the hydro-meteorological threshold identification, leading to TSS_{par} values up to 0.71, which were much higher than those obtained with the traditional approach (i.e., $TSS_{pl} = 0.50$). The application of the Principal Component Analysis to soil moisture data at various depths enables by-passing the problem of identifying the most influential soil layer on landslide triggering, without deteriorating significantly performance and keeping the thresholds simple (two-dimensional).

360 In real situations, the use of the reanalysis data is limited by the fact that they are made available to the public with a delay of some weeks from present. This delay is expected to be significantly reduced in the near future, in light of the increasing computational capabilities. Furthermore, our study corroborates with real data the potential improvements of the prediction capabilities of landslide triggering thresholds that use soil moisture information, which can be even greater with more accurate in-situ distributed soil moisture measurements. In this regard,

365 given the appreciable improvements obtained despite the inherent uncertainty of the reanalysis global dataset, future perspectives will involve the identification of the proposed hydro-meteorological thresholds using surface soil moisture products with enhanced spatial and temporal resolution (i.e., in situ measurements, reanalysis and satellite soil moisture data provided at real or near real time). Finally, our study will evaluate, in the near future, the applicability of the proposed methodology to other climate regions than the Mediterranean one, in order to

370 assess, more in depth, the potentialities of the presented results.

Authors' contributions. Conceptualization, N.P., D.J.P., E.C. and A.C.; formal analysis, N.P. and D.J.P.; investigation, N.P. and D.J.P.; methodology, N.P. and D.J.P.; coding, N.P. and D.J.P.; supervision, D.J.P., E.C. and A.C.; writing original draft, N.P. and D.J.P.; writing, review and editing, N.P., D.J.P., E.C. and A.C. All authors have read and agreed to the published version of the manuscript.

375 **Data availability**. FraneItalia landslides catalogue (Calvello and Pecoraro, 2018) is available at https://franeitalia.wordpress.com/database/ (last accessed on 16/06/2022). Rainfall measurements are available at websites of the Servizio Informativo Agrometeorologico Siciliano (SIAS) (http://www.sias.regione.sicilia.it/, last accessed on 16/06/2022) and at the Osservatorio delle Acque (http://www.acq.isprambiente.it/annalipdf/, ISPRA, 2020 – for Sicily, last accessed on 16/06/2022). Reanalysis soil moisture data are available from
380 https://cds.climate.copernicus.eu/cdsapp#!/dataset/reanalysis-era5-land?tab=form (last accessed on 16/06/2022).

Acknowledgements. Nunziarita Palazzolo doctoral program's grant is funded by University of Pavia. Research partially carried out within the project HydrEx – Hydrological extremes in a changing climate – Piano di incentivi per la ricerca di Ateneo (Pia.ce.ri.), 2020-2022, Università di Catania. APCs funded by "Fondi di Ateneo 2020-2022, Università di Catania, linea Open Access".

385 **References**

Abdi, H. and Williams, L. J.: Principal component analysis, Wiley Interdiscip. Rev. Comput. Stat., 2, 433–459, https://doi.org/10.1002/WICS.101, 2010.

Alecci, S. and Rossi, G.: Controllo di qualità dei dati pluviometrici ed analisi delle serie temporali, Siccità. Anal. Monit. e mitigazione. Appl. Sicil. Nuova Ed. Bios, Cosenza, Ital., 2007.

390 Aleotti, P.: A warning system for rainfall-induced shallow failures, Eng. Geol., 73, 247–265, https://doi.org/10.1016/j.enggeo.2004.01.007, 2004.

Beck, H. E., Pan, M., Miralles, D. G., Reichle, R. H., Dorigo, W. A., Hahn, S., Sheffield, J., Karthikeyan, L., Balsamo, G., Parinussa, R. M., van Dijk, A. I. J. M., Du, J., Kimball, J. S., Vergopolan, N., and Wood, E. F.: Evaluation of 18 satellite-And model-based soil moisture products using in situ measurements from 826 sensors, Hydrol. Earth Syst. Sci., 25, 17–40,
395 https://doi.org/10.5194/hess-25-17-2021, 2021.

Berti, M., Martina, M. L. V., Franceschini, S., Pignone, S., Simoni, A., and Pizziolo, M.: Probabilistic rainfall thresholds for landslide occurrence using a Bayesian approach, J. Geophys. Res. Earth Surf., 117, 1–20, https://doi.org/10.1029/2012JF002367, 2012.

Bogaard, T. and Greco, R.: Invited perspectives: Hydrological perspectives on precipitation intensity-duration thresholds for
400 landslide initiation: Proposing hydro-meteorological thresholds, Nat. Hazards Earth Syst. Sci., 18, 31–39,
https://doi.org/10.5194/nhess-18-31-2018, 2018.

Bogaard, T. A. and Greco, R.: Landslide hydrology: from hydrology to pore pressure, Wiley Interdiscip. Rev. Water, 3, 439–
459, https://doi.org/10.1002/wat2.1126, 2016.

Brocca, L., Ciabatta, L., Moramarco, T., Ponziani, F., Berni, N., and Wagner, W.: Use of Satellite Soil Moisture Products for
405 the Operational Mitigation of Landslides Risk in Central Italy, Elsevier Inc., 231–247 pp., https://doi.org/10.1016/B978-0-
12-803388-3.00012-7, 2016.

Brunetti, M. T., Peruccacci, S., Rossi, M., Luciani, S., Valigi, D., and Guzzetti, F.: Rainfall thresholds for the possible
occurrence of landslides in Italy, Nat. Hazards Earth Syst. Sci., 10, 447–458, https://doi.org/10.5194/nhess-10-447-2010,
2010.

410 Calvello, M. and Pecoraro, G.: FraneItalia: a catalog of recent Italian landslides, 5, https://doi.org/10.1186/s40677-018-0105-
5, 2018.

Chae, B.-G., Park, H.-J., Catani, F., Simoni, A., and Berti, M.: Landslide prediction, monitoring and early warning: a concise
review of state-of-the-art, 21, 1033–1070, https://doi.org/10.1007/s12303-017-0034-4, 2017.

Conrad, J. L., Morphew, M. D., Baum, R. L., and Mirus, B. B.: HydroMet: A new code for automated objective optimization
415 of hydrometeorological thresholds for landslide initiation, 13, https://doi.org/10.3390/w13131752, 2021.

Crozier, M. J.: Prediction of rainfall-triggered landslides: a test of the Antecedent Water Status Model, Earth Surf. Process.
Landforms, 24, 825–833, https://doi.org/https://doi.org/10.1002/(SICI)1096-9837(199908)24:9<825::AID-ESP14>3.0.CO;2-
M, 1999.

Crozier, M. J.: Deciphering the effect of climate change on landslide activity: A review, 124, 260–267,
420 https://doi.org/10.1016/J.GEOMORPH.2010.04.009, 2010.

Dijkstra, T. A. and Dixon, N.: Climate change and slope stability in the UK: challenges and approaches, Q. J. Eng. Geol.
Hydrogeol., 43, 371–385, https://doi.org/10.1144/1470-9236/09-036, 2010.

Distefano, P., Peres, D. J., Scandura, P., and Cancelliere, A.: Brief communication: Rainfall thresholds based on Artificial
neural networks can improve landslide early warning, https://doi.org/10.5194/nhess-2021-206, 2021.

425   Dorigo, W. A., Wagner, W., Hohensinn, R., Hahn, S., Paulik, C., Xaver, A., Gruber, A., Drusch, M., Mecklenburg, S., Van Oevelen, P., Robock, A., and Jackson, T.: The International Soil Moisture Network: A data hosting facility for global in situ soil moisture measurements, Hydrol. Earth Syst. Sci., 15, 1675–1698, https://doi.org/10.5194/hess-15-1675-2011, 2011.

Froude, M. J. and Petley, D. N.: Global fatal landslide occurrence from 2004 to 2016, Nat. Hazards Earth Syst. Sci., 18, 2161–2181, https://doi.org/10.5194/nhess-18-2161-2018, 2018.

430   Gain, A. K., Bühler, Y., Haegeli, P., Molinari, D., Parise, M., Peres, D. J., Pinto, J. G., Trigo, R. M., Llasat, M. C., and Kreibich, H.: Brief Communication : Key papers of 20 years in Natural Hazards and Earth System Sciences, 1–13, 2021.

Gariano, S. L. and Guzzetti, F.: Landslides in a changing climate, Earth-Science Rev., 162, 227–252, https://doi.org/10.1016/J.EARSCIREV.2016.08.011, 2016.

Gariano, S. L., Brunetti, M. T., Iovine, G., Melillo, M., Peruccacci, S., Terranova, O., Vennari, C., and Guzzetti, F.:
435   Calibration and validation of rainfall thresholds for shallow landslide forecasting in Sicily, southern Italy, 228, 653–665, https://doi.org/10.1016/j.geomorph.2014.10.019, 2015.

Guzzetti, F., Peruccacci, S., Rossi, M., and Stark, C. P.: Rainfall thresholds for the initiation of landslides in central and southern Europe, Meteorol. Atmos. Phys., 98, 239–267, https://doi.org/10.1007/s00703-007-0262-7, 2007a.

Guzzetti, F., Peruccacci, S., Rossi, M., and Stark, C. P.: Rainfall thresholds for the initiation of landslides in central and
440   southern Europe, Meteorol. Atmos. Phys., 98, 239–267, https://doi.org/10.1007/s00703-007-0262-7, 2007b.

Guzzetti, F., Peruccacci, S., Rossi, M., and Stark, C. P.: The rainfall intensity-duration control of shallow landslides and debris flows: An update, 5, 3–17, https://doi.org/10.1007/s10346-007-0112-1, 2008.

Hersbach, H., Bell, B., Berrisford, P., Hirahara, S., Horányi, A., Muñoz-Sabater, J., Nicolas, J., Peubey, C., Radu, R., Schepers, D., Simmons, A., Soci, C., Abdalla, S., Abellan, X., Balsamo, G., Bechtold, P., Biavati, G., Bidlot, J., Bonavita,
445   M., De Chiara, G., Dahlgren, P., Dee, D., Diamantakis, M., Dragani, R., Flemming, J., Forbes, R., Fuentes, M., Geer, A., Haimberger, L., Healy, S., Hogan, R. J., Hólm, E., Janisková, M., Keeley, S., Laloyaux, P., Lopez, P., Lupu, C., Radnoti, G., de Rosnay, P., Rozum, I., Vamborg, F., Villaume, S., and Thépaut, J. N.: The ERA5 global reanalysis, Q. J. R. Meteorol. Soc., 146, 1999–2049, https://doi.org/10.1002/qj.3803, 2020.

Highland, L. M. and Bobrowsky, P.: The landslide Handbook - A guide to understanding landslides, US Geol. Surv. Circ.,
450   1–147, https://doi.org/10.3133/cir1325, 2008.

Jolliffe, I. T.: Principal component analysis for special types of data, Springer New York, (pp. 338-372). pp., 2002.

Kherif, F. and Latypova, A.: Principal component analysis, Mach. Learn. Methods Appl. to Brain Disord., 209–225, https://doi.org/10.1016/B978-0-12-815739-8.00012-2, 2019.

Li, M., Wu, P., and Ma, Z.: A comprehensive evaluation of soil moisture and soil temperature from third-generation atmospheric and land reanalysis data sets, Int. J. Climatol., 40, 5744–5766, https://doi.org/10.1002/joc.6549, 2020.

Marino, P., Peres, D. J., Cancelliere, A., Greco, R., and Bogaard, T. A.: Soil moisture information can improve shallow landslide forecasting using the hydrometeorological threshold approach, 17, 2041–2054, https://doi.org/10.1007/s10346-020-01420-8, 2020.

McInnes, R., Jakeways, J., Fairbank, H., and Mathie, E.: Landslides and Climate Change: Challenges and Solutions: Proceedings of the International Conference on Landslides and Climate Change, Ventnor, Isle of Wight, UK, 21-24 May 2007, CRC Press, 2007.

Melillo, M., Brunetti, M. T., Peruccacci, S., Gariano, S. L., Roccati, A., and Guzzetti, F.: A tool for the automatic calculation of rainfall thresholds for landslide occurrence, Environ. Model. Softw., 105, 230–243, https://doi.org/10.1016/j.envsoft.2018.03.024, 2018.

Mirus, B. B., Morphew, M. D., and Smith, J. B.: Developing Hydro-Meteorological Thresholds for Shallow Landslide Initiation and Early Warning, Water 2018, Vol. 10, Page 1274, 10, 1274, https://doi.org/10.3390/W10091274, 2018a.

Mirus, B. B., Becker, R. E., Baum, R. L., and Smith, J. B.: Integrating real-time subsurface hydrologic monitoring with empirical rainfall thresholds to improve landslide early warning, 15, 1909–1919, https://doi.org/10.1007/s10346-018-0995-z, 2018b.

Palau, R. M., Hürlimann, M., Berenguer, M., and Sempere-Torres, D.: Towards the use of hydrometeorological thresholds for the regional-scale LEWS of Catalonia (NE Spain)., https://doi.org/10.5194/EGUSPHERE-EGU21-8221, 2021.

Peirce, C. S.: The numerical measure of the success of predictions., Science, 4, 453–454, https://doi.org/10.1126/science.ns-4.93.453-a, 1884.

Peres, D. J. and Cancelliere, A.: Derivation and evaluation of landslide-triggering thresholds by a Monte Carlo approach, Hydrol. Earth Syst. Sci., 18, 4913–4931, https://doi.org/10.5194/hess-18-4913-2014, 2014.

Peres, D. J. and Cancelliere, A.: Modeling impacts of climate change on return period of landslide triggering, J. Hydrol., 567, 420–434, https://doi.org/10.1016/j.jhydrol.2018.10.036, 2018.

Peres, D. J. and Cancelliere, A.: Comparing methods for determining landslide early warning thresholds: potential use of non-triggering rainfall for locations with scarce landslide data availability, 18, 3135–3147, https://doi.org/10.1007/s10346-021-01704-7, 2021.

Ponziani, F., Pandolfo, C., Stelluti, M., Berni, N., Brocca, L., and Moramarco, T.: Assessment of rainfall thresholds and soil moisture modeling for operational hydrogeological risk prevention in the Umbria region (central Italy), 9, 229–237, https://doi.org/10.1007/s10346-011-0287-3, 2012.

Postance, B., Hillier, J., Dijkstra, T., and Dixon, N.: Comparing threshold definition techniques for rainfall-induced landslides: A national assessment using radar rainfall, Earth Surf. Process. Landforms, 43, 553–560, https://doi.org/10.1002/ESP.4202, 2018.

Pumo, D., Carlino, G., Blenkinsop, S., Arnone, E., Fowler, H., and Noto, L. V.: Sensitivity of extreme rainfall to temperature in semi-arid Mediterranean regions, Atmos. Res., 225, 30–44, https://doi.org/10.1016/j.atmosres.2019.03.036, 2019.

Reder, A. and Rianna, G.: Exploring ERA5 reanalysis potentialities for supporting landslide investigations: a test case from Campania Region (Southern Italy), 18, 1909–1924, https://doi.org/10.1007/S10346-020-01610-4/FIGURES/11, 2021.

Rencher, A. C.: Multivariate statistical inference and applications, Wiley-Interscience, 1998.

Roccati, A., Faccini, F., Luino, F., Ciampalini, A., and Turconi, L.: Heavy rainfall triggering shallow landslides: A susceptibility assessment by a GIS-approach in a Ligurian Apennine catchment (Italy), 11, https://doi.org/10.3390/w11030605, 2019.

Roccati, A., Paliaga, G., Luino, F., Faccini, F., and Turconi, L.: Rainfall threshold for shallow landslides initiation and analysis of long-term rainfall trends in a mediterranean area, https://doi.org/10.3390/atmos11121367, 2020.

Segoni, S., Piciullo, L., and Gariano, S. L.: A review of the recent literature on rainfall thresholds for landslide occurrence, https://doi.org/10.1007/s10346-018-0966-4, 1 August 2018a.

Segoni, S., Piciullo, L., and Gariano, S. L.: A review of the recent literature on rainfall thresholds for landslide occurrence, 15, 1483–1501, https://doi.org/10.1007/s10346-018-0966-4, 2018b.

Segoni, S., Rosi, A., Lagomarsino, D., Fanti, R., and Casagli, N.: Brief communication: Using averaged soil moisture estimates to improve the performances of a regional-scale landslide early warning system, Nat. Hazards Earth Syst. Sci., 18, 807–812, https://doi.org/10.5194/NHESS-18-807-2018, 2018c.

Staley, D. M., Kean, J. W., Cannon, S. H., Schmidt, K. M., and Laber, J. L.: Objective definition of rainfall intensity-
505   duration thresholds for the initiation of post-fire debris flows in southern California, 10, 547–562,
https://doi.org/10.1007/s10346-012-0341-9, 2013.

Thomas, M. A., Mirus, B. B., and Collins, B. D.: Identifying Physics-Based Thresholds for Rainfall-Induced Landsliding,
Geophys. Res. Lett., 45, 9651–9661, https://doi.org/10.1029/2018GL079662, 2018.

Thomas, M. A., Collins, B. D., and Mirus, B. B.: Assessing the Feasibility of Satellite-Based Thresholds for Hydrologically
510   Driven Landsliding, Water Resour. Res., 55, 9006–9023, https://doi.org/10.1029/2019WR025577, 2019.

Venturella, G.: Climatic and pedological features of Sicily, 17, 47–53, 2004.

Wicki, A., Lehmann, P., Hauck, C., Seneviratne, S. I., Waldner, P., and Stähli, M.: Assessing the potential of soil moisture
measurements for regional landslide early warning, 17, 1881–1896, https://doi.org/10.1007/s10346-020-01400-y, 2020a.

Wicki, A., Lehmann, P., Hauck, C., Seneviratne, S. I., Waldner, P., and Stähli, M.: Assessing the potential of soil moisture
515   measurements for regional landslide early warning, 17, 1881–1896, https://doi.org/10.1007/S10346-020-01400-
Y/FIGURES/11, 2020b.

Wicki, A., Jansson, E., Lehmann, P., Hauck, C., and Stähli, M.: Simulated or measured soil moisture: which one is adding
more value to regional landslide early warning?, Hydrol. Earth Syst. Sci, 25, 4585–4610, https://doi.org/10.5194/hess-25-
4585-2021, 2021.

520   Zhao, B., Dai, Q., Han, D., Dai, H., Mao, J., and Zhuo, L.: Probabilistic thresholds for landslides warning by integrating soil
moisture conditions with rainfall thresholds, J. Hydrol., 574, 276–287, https://doi.org/10.1016/j.jhydrol.2019.04.062, 2019.